Available online at www.eccomasproceedia.org
Eccomas Proceedia COMPDYN (2021) 4508-4519

ECCOMAS
Proceedia

COMPDYN 2021
8th ECCOMAS Thematic Conference on
Computational Methods in Structural Dynamics and Earthquake Engineering
M. Papadrakakis, M. Fragiadakis (eds.)
Streamed from Athens, Greece, 28 - 30 June 2021

EFFICIENT DAMPER DESIGN METHOD FOR ELASTIC-PLASTIC MDOF STRUCTURES UNDER CONSECUTIVE-LEVEL EARTHQUAKES

H. Akehashi[1], **I. Takewaki**[2]

[1] Graduate student, Dept of Architecture and Architectural Engineering, Kyoto University
Kyoto University, Kyoto 615-8540, Japan
e-mail: fm-akehashi@archi.kyoto-u.ac.jp

[2] Professor, Dept of Architecture and Architectural Engineering, Kyoto University
Kyoto University, Kyoto 615-8540, Japan
takewaki@archi.kyoto-u.ac.jp

Abstract

A new optimal damper design method, called 'consecutive design generation method (CDGM)', is presented for elastic-plastic multi-degree-of-freedom (MDOF) building structures under multiple-level earthquake ground motions (GMs). The procedure of the proposed method is as follows: (i) Set a variety of levels of input GMs $\{IM_1,\ldots,IM_L\}$ $(IM_1 < \ldots < IM_L)$. *(ii) Obtain the optimal design under GM with* $IM = IM_1$ *using an optimization method. (iii) Obtain the optimal design under GM with* $IM = IM_2$ *by a local search around the optimal design under GM with* $IM = IM_1$ *as the initial design. (iv) Obtain the optimal design under GM with* $IM = IM_3$ *by a local search around the optimal design under GM with* $IM = IM_2$ *as the initial design, and the same procedure is repeated under GMs with other IMs. By using the proposed method, all the optimal designs can be obtained with much lower computational effort than the method repeating an ordinary optimization procedure under every-level GM. The proposed method helps to understand how the distribution of added damper damping coefficients changes as the level of GMs changes. Furthermore, a simple design guideline for the problem, which design to be chosen from various optimal designs, is presented based on the 'ideal drift response curve', which is also a new concept. Two representative recorded ground motions are employed as a set of GMs and the proposed method is applied to these GMs. The influence of the number of GMs and the level of GMs on the optimal damper design is clarified.*

Keywords: Earthquake response, Elastic-plastic response, Seismic design, Viscous damping, Optimal damper placement, Robust design.

ISSN:2623-3347
Peer-review under responsibility of the organizing committee of COMPDYN 2021.
doi: 10.7712/120121.8803.19124

1 INTRODUCTION

Problems of optimal design of passive dampers have been tackled by many researchers (for example see [6, 11]). Zhang and Soong [15] proposed a sequential procedure to obtain the optimal placement of viscoelastic dampers. Then this method was extended to a simpler method by Garcia [5]. Takewaki [10] developed an optimality criteria-based algorithm to minimize the sum of the amplitudes of the transfer functions at the fundamental natural frequency under a constraint on the sum of the additional damping coefficients. Silvestri and Trombetti [9] demonstrated the effectiveness of mass-proportional damping systems. Some researchers compared several methods for optimal damper placement ([2, 4, 14]).

In most researches on optimal damper placement, elastic frames are treated and a limited number of researches deal with optimal damper placement problems for inelastic frames (for example, [1, 7, 12]). In the presence of yielding in a frame, the setting of the level of input ground motions (GMs) used for the optimization affects the final design. However, even in these studies, a problem how to determine the level of input GMs has not been examined. An optimal damper distribution designed under a specified-level GM may not be necessarily effective for larger-level GMs. Especially, a model optimally designed in the elastic range exhibits a large plastic deformation concentration to specific stories for larger inputs [2, 3]. Therefore, a design effective for various levels of GMs is desirable.

In this paper, a new optimal damper design method, called a 'consecutive design generation method (CDGM)', is presented for elastic-plastic multi-degree-of-freedom (MDOF) building structures under multiple-level GMs. The procedure of the proposed method is as follows: (i) Set a variety of levels of input GMs $\{IM_1,...,IM_L\}$ $(IM_1 < ... < IM_L)$. (ii) Obtain the optimal design under GM with $IM = IM_1$ using an optimization method. (iii) Obtain the optimal design under GM with $IM = IM_2$ by a local search around the optimal design under GM with $IM = IM_1$ as the initial design. (iv) Obtain the optimal design under GM with $IM = IM_3$ by a local search around the optimal design under GM with $IM = IM_2$ as the initial design, and the same procedure is repeated under GMs with other *IM*s. By using the proposed method, all the optimal designs can be obtained with much lower computational effort than the method repeating an ordinary optimization procedure under every-level GM. The proposed method helps to understand how the distribution of added damper damping coefficients changes as the level of GMs changes. Furthermore, a simple design guideline for the problem, which design to be chosen from various optimal designs, is presented based on the 'ideal drift response curve', which is also a new concept. Two representative recorded ground motions are employed as a set of GMs and the proposed method is applied to these GMs. The influence of the number of GMs and the level of GMs on the optimal damper design is clarified.

2 PROBLEM OF OPTIMAL DAMPER PLACEMENT

In this section, two kinds of problems of optimal damper placement are presented. An ordinary problem of optimal damper placement (OPODP) is stated as minimizing the maximum interstory drift under the condition on the specified total quantity of added viscous damping coefficients and the specified level of input GMs. Another problem is to find the problem of optimal damper placements under consecutive-level GMs (PODPCG). The problem PODPCG is mainly dealt with in this paper. Since elastic-plastic MDOF structures are dealt with, the setting of the level of input GMs affects the final design. Therefore, solving the problem PODPCG helps to understand how the distribution of added damper damping coefficients changes as the level of GMs increases. The relation of the problems OPODP and PODPCG will be explained, and a solution algorithm will be proposed for the problem PODPCG.

2.1 Problem of optimal damper placement for consecutive-level ground motions

Consider first the problem OPODP.

[Ordinary Problem of Optimal Damper Placement (OPODP)]

$$\begin{aligned}&\textit{Find } \mathbf{c}_{add}\\&\textit{so as to minimize } d_{\max} = \max_i\{d_{\max,i}\}\\&\textit{subject to } \mathbf{c}_{add}\cdot\mathbf{1} = W_c \ (const.)\end{aligned}$$

where $\mathbf{c}_{add}, d_{\max,i}, W_c$ denote the added damping coefficient vector, the maximum interstory drift in the i-th story, the sum of the added damping coefficients, respectively.

Consider next the problem PODPCG.

[Problem of Optimal Damper Placements for Consecutive-level GMs (PODPCG)]

Obtain the L *sets of damper placements* $\mathbf{c}_{add}^{opt}(IM_1),...,\mathbf{c}_{add}^{opt}(IM_L)$ $(IM_1 < ... < IM_L)$

where $IM, L, \mathbf{c}_{add}^{opt}(IM_j)$ denote the level of input GMs, the number of IMs, the optimal damper placement under the GMs with $IM = IM_j$, respectively.

All the optimal designs $\mathbf{c}_{add}^{opt}(IM_1),...,\mathbf{c}_{add}^{opt}(IM_L)$ are obtained by solving the problem OPODP L times for each level of the input GMs. However, it is preferable to avoid such iteration for lower computational effort. To overcome this difficulty, a simple and efficient approach including a local search is proposed.

2.2 Solution algorithm: consecutive design generation method

The solution algorithm for the problem PODPCG may be described as follows.

[Algorithm: Consecutive Design Generation Method (CDGM)]

Step 1 Set a variety of levels of input GMs $\{IM_1,...,IM_L\}$ $(IM_1 < ... < IM_L)$.

Step 2 Obtain $\mathbf{c}_{add}^{opt}(IM_1)$ using an optimization method. Put $i \to 1$.

Step 3 Obtain $\mathbf{c}_{add}^{opt}(IM_{i+1})$ by a local search around $\mathbf{c}_{add}^{opt}(IM_i)$ as the initial design.

- 3.1 Find the story *j* which exhibits the largest value of $d_{\max,j}$.
- 3.2 Select the stories in which dampers are installed (exclude the stories without damper). Then find the story *k* which exhibits the minimum value of $d_{\max,k}$ from those stories.
- 3.3 Update the damping coefficients $c_j \to c_j + \Delta c, c_k \to c_k - \Delta c$.
- 3.4 Repeat 3.1-3.3 n_{ls} times.
- 3.5 Select the design which exhibits the minimum value of $d_{\max}$ from n_{ls} designs.

Step 4 Put $i \to i+1$. If $i = L$ is satisfied, then finalize the process. If $i < L$ is satisfied, return to Step 3.

The overview and the flow of this algorithm are shown in Figure 1. It is noted that the sensitivity-based approach [3, 8] is adopted to obtain $\mathbf{c}_{add}^{opt}(IM_1)$ in this paper. It is also pointed out that the local search method used in Step 3, 4 is quite simple, but it works well so far as the value of $\Delta IM (= IM_{i+1} - IM_i)$ is small (the effectiveness of the proposed local search method is demonstrated through the numerical examples in Section 3.1 and 3.2).

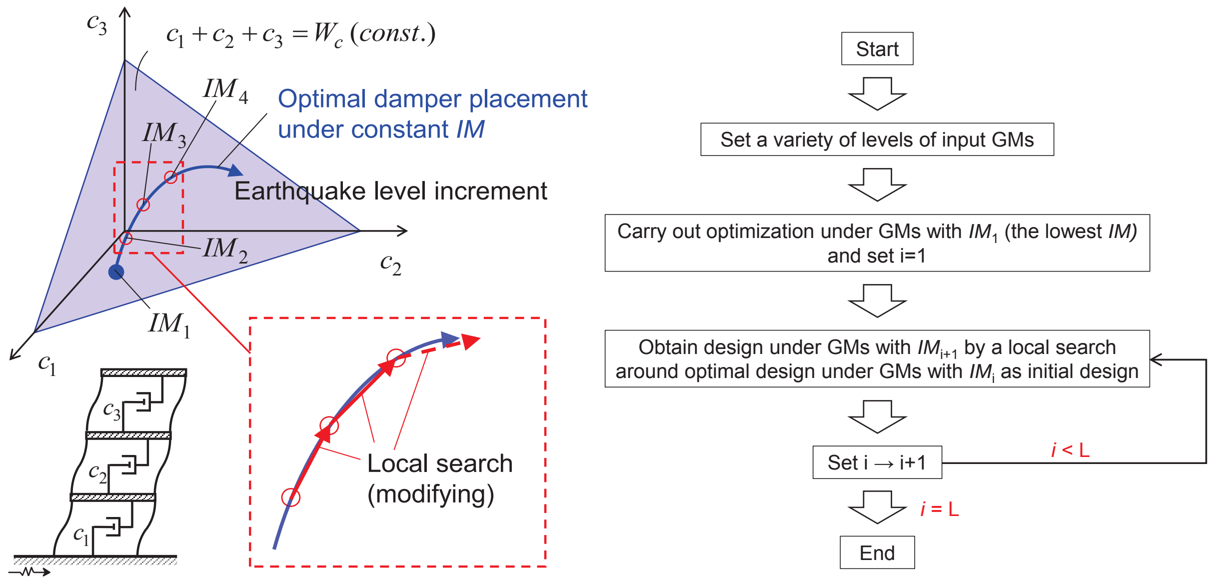

Figure 1: Overview and schematic diagram of proposed solution algorithm.

NUMERICAL EXAMPLE

Consider two shear building models of 12 stories with different story stiffness distributions. Model 1 has a trapezoidal distribution of story stiffnesses ($(k_1/k_{12})=4$). Model 2 has a uniform distribution of story stiffnesses. The undamped fundamental natural period of these two models is 1.2[s] and the structural damping ratio is 0.01 (stiffness proportional type). All the floor masses have the same value. The common story height is 4[m] and the common yield interstory drift is 4/150[m]. The story shear-interstory drift relation obeys the elastic perfectly-plastic rule.

2.3 Influence of level of input ground motion

In this section, the influence of the level of input GMs on the final design is investigated. El Centro NS component during the Imperial Valley earthquake in 1940 is employed here. The level of the GM is adjusted by the peak ground velocities (PGV). 51 levels of the GM (from PGV =0.5 [m/s] to PGV =1.5 [m/s] by the increment 0.02 [m/s]) are used to obtain the optimal designs. The sensitivity-based approach [3, 8] is adopted to obtain $\mathbf{c}_{add}^{opt}(\mathrm{PGV}{=}0.5)$ and the required number of time-history response analyses is about 6000 to obtain $\mathbf{c}_{add}^{opt}(\mathrm{PGV}{=}0.5)$. The targeted value of the sum of the added damping coefficients is set to $W_c=10\times10^7[\mathrm{Ns/m}]$. The value of W_c is given so that the final design has the fundamental-mode damping ratio of about 0.05. $n_{ls}=50$ and $\Delta c=W_c/240$ are employed for the local search. The total number of time-history response analyses is $6000+n_{ls}\times(51-1)=8500$.

Figures 2 and 3 show the optimal designs for Model 1 and 2. It can be observed that the proposed method certainly provides effective designs for various levels of GMs for both Model 1, 2. This means that the proposed local search method works well even though the local search method is quite simple. It can also be said that, as PGV used for the design becomes larger, the dampers concentrated to the specified stories spread around those stories and the distributions of added damping coefficients become smoother. This is because those surrounding stories without dampers tend to exhibit large deformation concentrations for larger levels of GMs. For Model 1, the added dampers are allocated only in the 6-10th stories in the case of $\mathrm{PGV} < 0.7[\mathrm{m/s}]$. As PGV becomes larger, the dampers are allocated to the 4-5th stories. For Model 2, the dampers allocated only in the 1-3th stories for smaller PGV spread to the 4-6th stories as PGV becomes larger. Furthermore, the distribution of added damping coefficients shows a drastic change just after d_{max} / d_y attains 1 as shown in Figures 2c and 3c. For larger levels of GMs, the distribution changes gently.

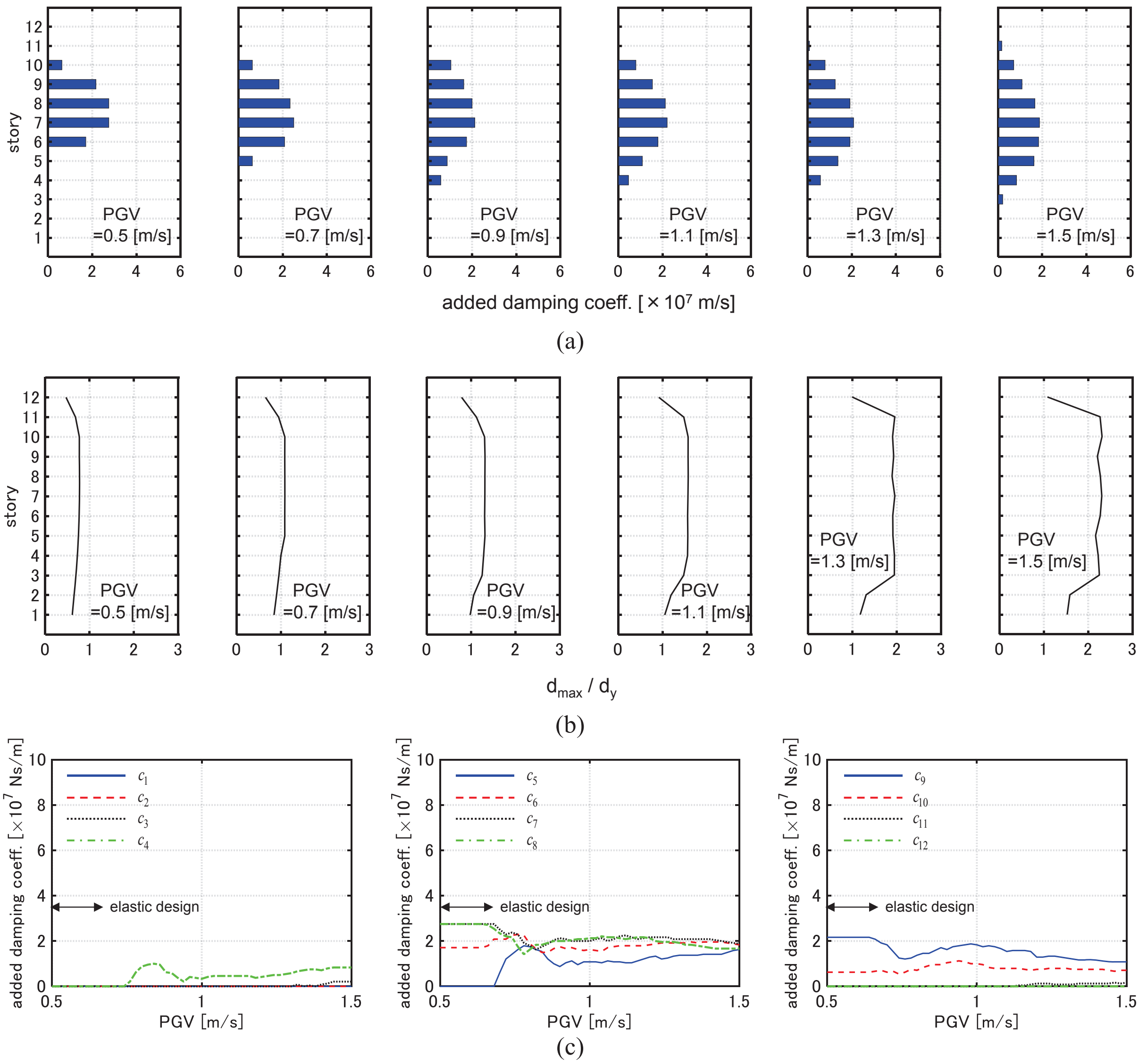

Figure 2: Optimal designs of added viscous damper for multiple-level GMs (Model 1), (a) distribution of added damping coefficient, (b) distribution of $d_{max,i} / d_y$, (c) change of added damping coefficient of each story.

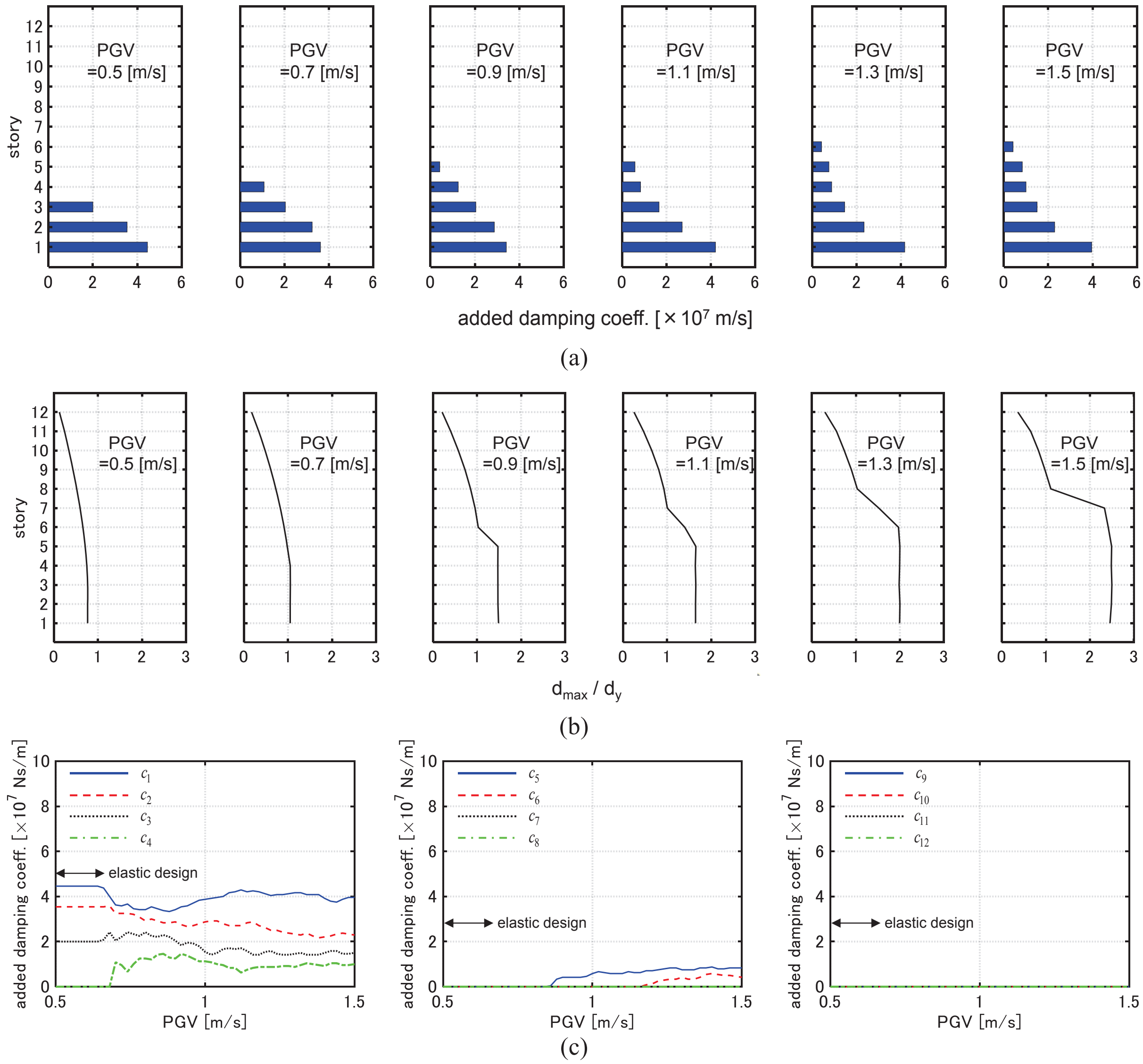

Figure 3: Optimal designs of added viscous damper for multiple-level GMs (Model 2), (a) distribution of added damping coefficient, (b) distribution of $d_{\max,i} / d_y$, (c) change of added damping coefficient of each story.

2.4 Influence of number of input ground motions

In this section, the influence of the number of input GMs on the final design is investigated. Hachinohe NS component during the Tokachi-oki earthquake in 1968 and El Centro NS component are employed. All the other parameters for the optimization are the same as those in Section 3.1. It should be noted that the predominant period of Hachinohe NS component is longer than that of El Centro NS component.

Figures 4 and 5 show the optimal designs for Model 1 and 2. It can be observed that, in the case of $\mathrm{PGV} \leq 0.9[\mathrm{m/s}]$, the optimal distributions of added damping coefficients are the same as those in Section 3.1. This is because El Centro NS component provides the response envelopes. When PGV used for the design becomes larger, Hachinohe NS component is critical in the lower stories. This means that, as PGV becomes large and the plastic deformation level increases, the equivalent natural period is lengthened. For Model 1, the distributions of the added damping coefficients are smoother than the optimal distributions designed only under El Centro NS component. For Model 2, similar to the case in Section 3.1, the added dampers are concentrated to the lower stories. This is because Model 2 has a uniform distribution of story stiffnesses and tends to exhibits plastic deformation concentration in the lower stories for large inputs. It can also be said that, while almost all the stories exhibit plastic deformations for large inputs in the case of Model 1, the upper stories remain elastic for large inputs in the case of Model 2. Therefore, the value of $d_{\max} / d_y$ of Model 2 for larger inputs are larger than that of Model 1.

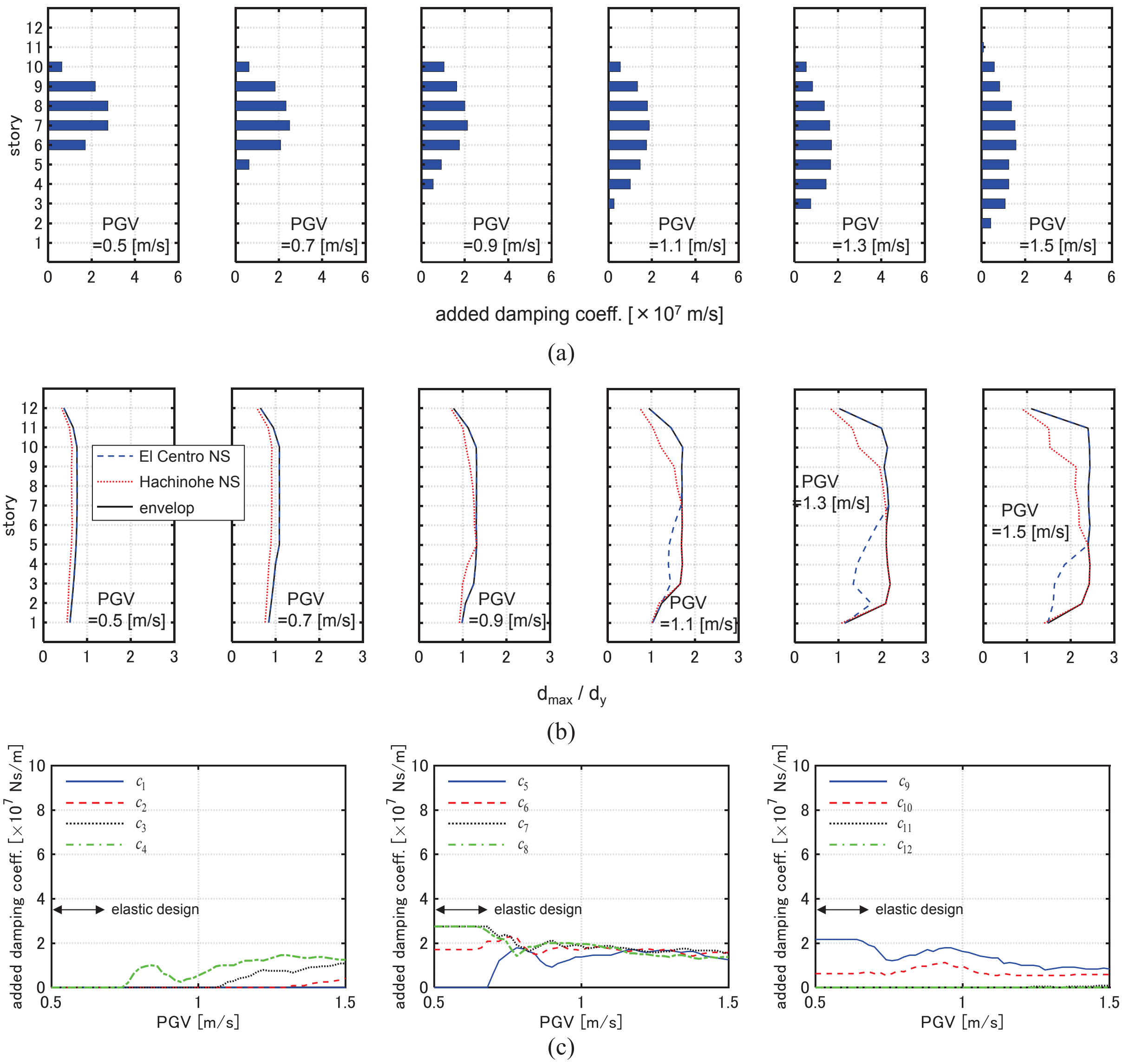

Figure 4: Optimal designs of added viscous damper for multiple-level two GMs (Model 1), (a) distribution of added damping coefficient, (b) distribution of $d_{\max,i} / d_y$, (c) change of added damping coefficient of each story.

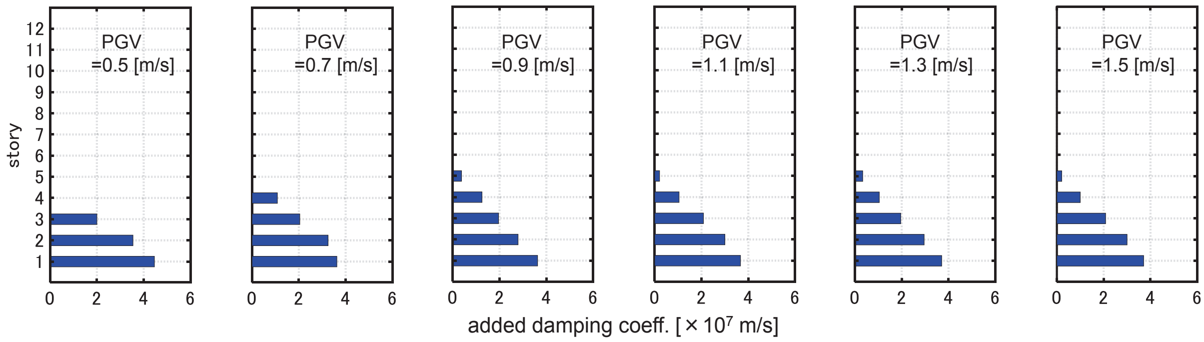

(a)

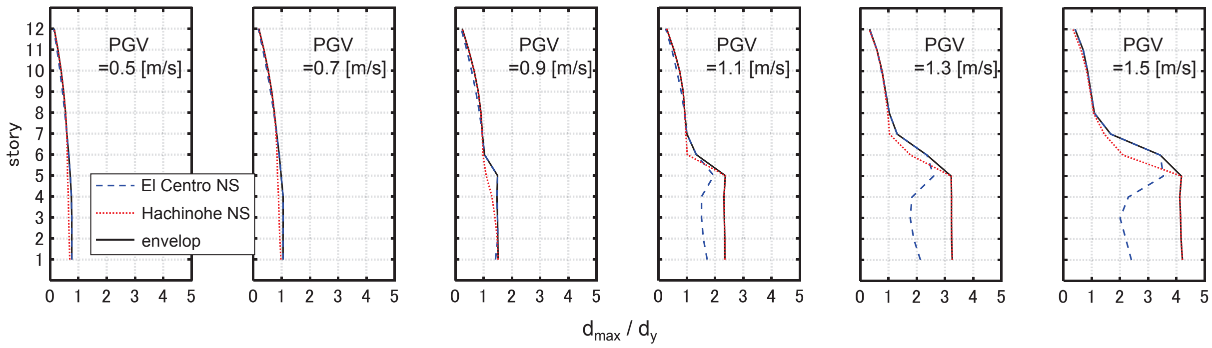

(b)

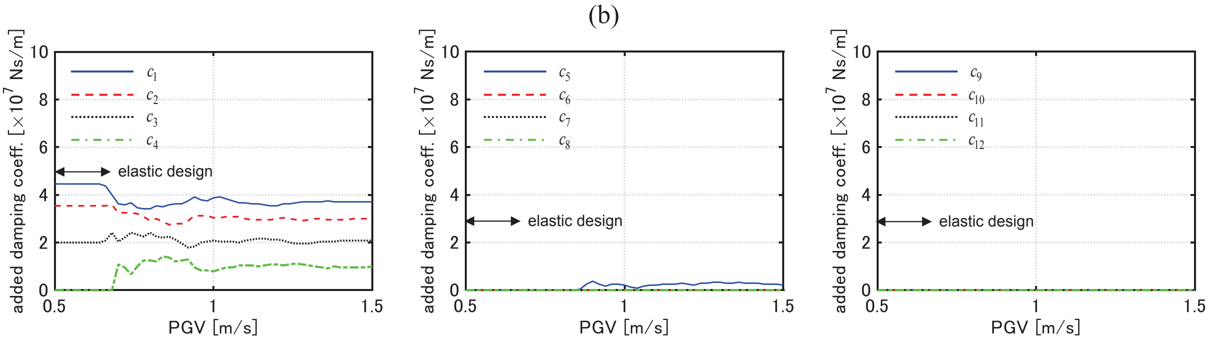

(c)

Figure 5: Optimal designs of added viscous damper for multiple-level two GMs (Model 2), (a) distribution of added damping coefficient, (b) distribution of $d_{\max,i} / d_y$, (c) change of added damping coefficient of each story.

2.5 IDA analysis and ideal drift response curve

In this section, IDA analysis [13] is conducted for the models obtained in Section 3.2. El Centro NS component and Hachinohe NS component are adopted for IDA. PGV is increased from 0.5 [m/s] to 1.5 [m/s] by 0.02 [m/s].

Figures 6a and 7a show the maximum interstory drift distributions by IDA analysis for the models designed under these two GMs with PGV=0.5, 1.0, 1.5 [m/s]. The input level PGV=0.5 corresponds to elastic design. It can be observed that the models designed for PGV=0.5, 1.0 [m/s] exhibits large deformation concentrations in specific stories for these two GMs with larger PGV. Figure 6c and 7c illustrate the critical earthquakes in the applications of IDA. El Centro NS component is critical in the lower range of PGV and Hachinohe NS component is critical in the upper range of PGV for all models since the predominant period of the latter is longer than that of the former as stated in Section 3.2.

Figures 6b and 7b show the IDA curves and the ideal drift response curves. An ideal drift response curve is a plot of the optimized maximum deformations versus design *IM*. The optimal designs for various levels of GMs are obtained by conducting CDGM, and simultaneously the ideal drift response curve is provided. The IDA curves for all the optimal designs never cross the ideal drift response curve, and the IDA curve for each optimal design is tangent to the ideal drift response curve only at the point where *IM* corresponds to the design *IM*. It can be observed that the IDA curves for the models designed for PGV=1.5 [m/s] run near the ideal drift response curves.

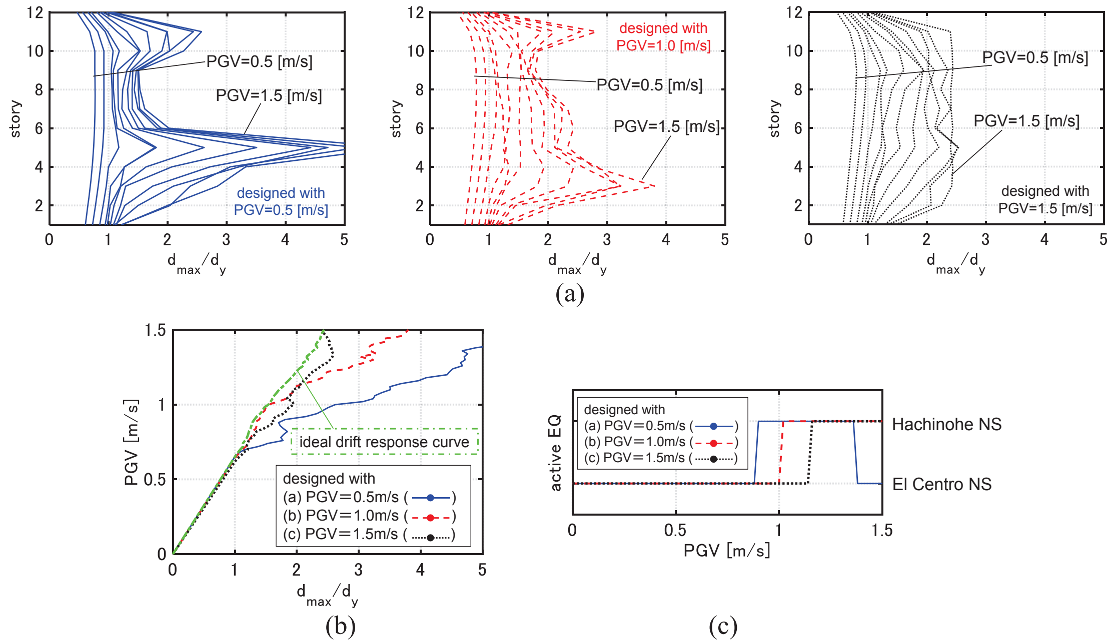

Figure 6: IDA analysis for 3 models designed under GMs with PGV=0.5, 1.0, 1.5 [m/s] (Model 1), (a) distribution of $d_{\max,i} / d_y$, (b) IDA curves and ideal drift response curve, (c) active EQ.

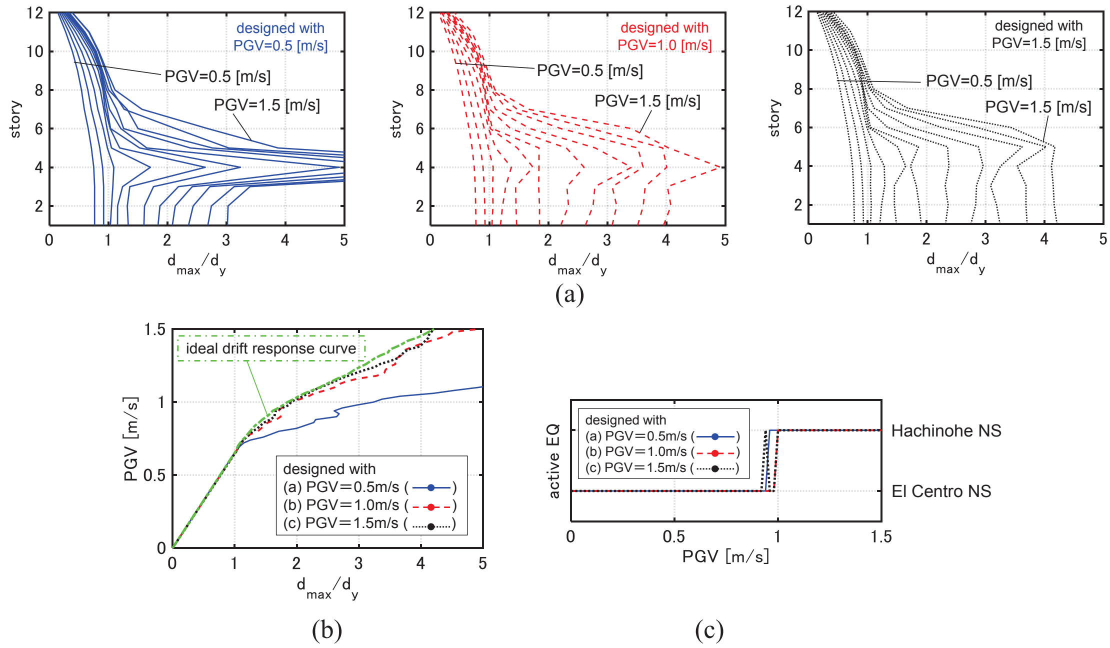

Figure 7: IDA analysis for 3 models designed under GMs with PGV=0.5, 1.0, 1.5 [m/s] (Model 2), (a) distribution of $d_{\max,i} / d_y$, (b) IDA curves and ideal drift response curve, (c) active EQ.

As shown in Figures 6 and 7, the model optimally designed for a specified-level GMs is not necessarily effective for other levels of GMs. Therefore, a design guideline for the problem, which design to be chosen from the various optimal designs, is needed. In this paper, a simple index for selection is introduced as follows,

$$\max_{IM}\{d_{\max}(IM)-\mathrm{IDRC}(IM)\}$$

where IDRC denotes the value of the ideal drift response curve. It can be said that the design, which minimizes the proposed index, shows high robustness (effective for various levels of GMs). Figure 8 indicates the procedure for selecting such design.

Figures 9 and 10 show the values of the proposed index for the models obtained in Section 3.2 and the IDA curves for the models which minimize the proposed index. It can be observed that, as PGV used for the design becomes larger, the value of the proposed index generally decreases. It can also be said that the elastic designs provide the highest value of the index. For both Models 1 and 2, the designs, which minimize the index, are effective for various levels of the GMs. Especially for Model 2, the IDA curve for the selected design runs quite near the ideal drift response curve. This is because Model 2 tends to exhibit plastic deformation concentration in the lower stories for large inputs as stated in Section 3.2.

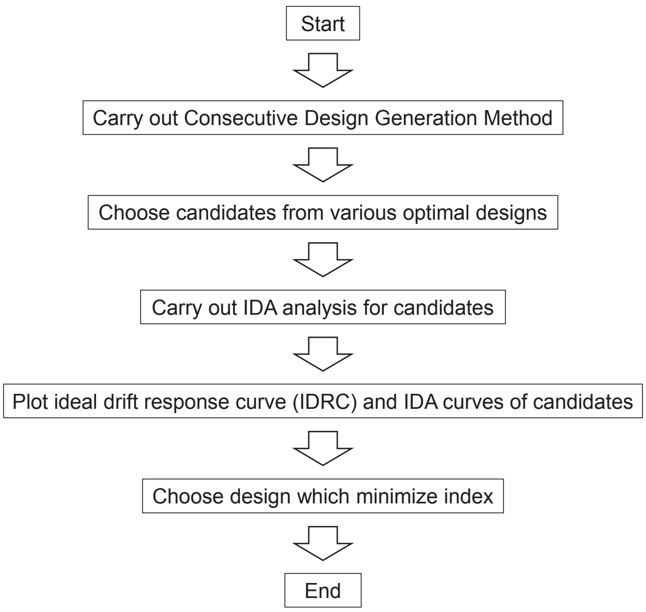

Figure 8: Schematic diagram for choosing robust design for various levels of GMs.

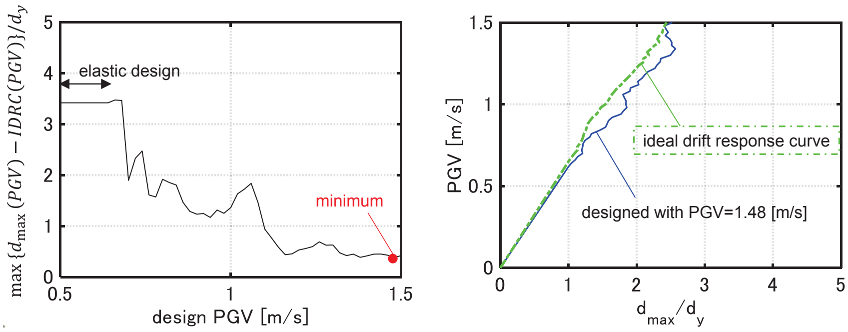

Figure 9: Proposed index and IDA curve for design with minimum index (Model 1).

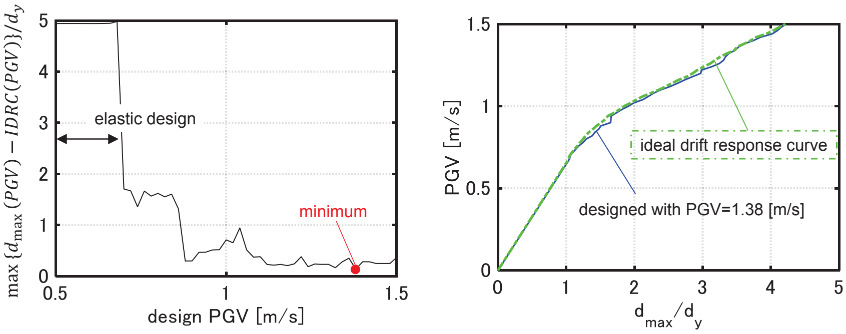

Figure 10: Proposed index and IDA curve for design with minimum index (Model 2).

3 CONCLUSIONS

A new optimal damper design method is presented for elastic-plastic MDOF building structures under multiple-level earthquake ground motions (GMs). The main conclusions can be summarized as follows.

- A consecutive design generation method (CDGM) was proposed for the above-mentioned problem. By using CDGM, all the optimal designs can be obtained with much lower computational effort than the method repeating an ordinary optimization procedure under every-level GM. CDGM also helps to understand how the distribution of added damper damping coefficients changes as the level of GMs changes.
- As the level of input GMs used for the design becomes larger, dampers concentrated to the specified stories spread around those stories and the distribution of the added damping coefficients becomes smoother.
- As the number of input GMs used for the design increases, the distribution of the added damping coefficients becomes smoother.
- Models designed for lower-level GMs may exhibit large plastic deformation concentrations in specific stories for larger-level GMs.
- A new concept of 'ideal drift response curve' was presented for selecting a robust design for various levels of GMs. This is a plot of the optimized maximum deformation versus design *IM* (level of input GMs). The optimal designs for various levels of GMs were obtained by conducting CDGM, and simultaneously the ideal drift response curve was provided.

REFERENCES

[1] Akehashi, H., and Takewaki, I. (2019). Optimal viscous damper placement for elastic-plastic MDOF structures under critical double impulse. *Frontiers in Built Environment*, 5: 20.

[2] Akehashi, H., and Takewaki, I. (2020a). Comparative investigation on optimal viscous damper placement for elastic-plastic MDOF structures: Transfer function amplitude or double impulse. *Soil Dyn. Earthq. Eng.*, 130, 105987.

[3] Akehashi, H., and Takewaki, I. (2020b). Simultaneous optimization of elastic-plastic building structures and viscous dampers under critical double impulse. *Frontiers in Built Environment*, 6, 211.

[4] Cetin, H., Aydin, E., and Ozturk, B. (2019). Optimal Design and Distribution of Viscous Dampers for Shear Building Structures under Seismic Excitations. *Frontiers in Built Environment*, 5: 90.

[5] Garcia, D.L. (2001). A simple method for the design of optimal damper configurations in MDOF structures. *Earthq. Spectra*, 17, 387-398.

[6] Lagaros, N. D. (Ed.). (2012) *Design optimization of active and passive structural control systems*., IGI Global.

[7] Lavan, O., and Avishur, M. (2013). Seismic behavior of viscously damped yielding frames under structural and damping uncertainties. *Bulletin of Earthq. Eng*., 11(6), 2309-2332.

[8] Murakami, Y., Noshi, K., Fujita, K., Tsuji, M., and Takewaki, I. (2013). Simultaneous optimal damper placement using oil, hysteretic and inertial mass dampers, *Earthq. and Struct*., 5(3), 261-276.

[9] Silvestri, S., and Trombetti, T. (2007). Physical and numerical approaches for the optimal insertion of seismic viscous dampers in shear-type structures. *J. Earthq. Eng*., 11, 787-828.

[10] Takewaki, I. (1997). Optimal damper placement for minimum transfer functions, *Earthq. Eng. Struct. Dyn*., 26(11), 1113-1124.

[11] Takewaki, I. (2009). *Building Control with Passive Dampers: -Optimal Performance-based Design for Earthquakes-*, John Wiley & Sons Ltd. (Asia), Singapore.

[12] Takewaki, I., and Akehashi, H. (2021). Comprehensive review of optimal and smart design of nonlinear building structures with and without passive dampers subjected to earthquake loading. *Frontiers in Built Environment*, 7: 631114.

[13] Vamvatsikos, D., and Cornell, C.A. (2001). Incremental dynamic analysis. *Earthq. Eng. Struct. Dyn*., 31(3), 491–514.

[14] Whittle, J.K., Williams, M.S., Karavasilis, T.L., and Blakeborough, A. (2012). A comparison of viscous damper placement methods for improving seismic building design, *J. Earthq. Eng*., 16(4), 540-560.

[15] Zhang, R. H., and Soong, T. T. (1992). Seismic design of viscoelastic dampers for structural applications. *J. Struct. Eng*., 118(5), 1375-1392.